Rotor Fault Diagnosis Based on Weighted D-S Evidence Theory

GAO Yadong*, *ZHANG Chuanzhuang*

College of Aerospace Engineering, Nanjing University of Aeronautics and Astronautics, Nanjing 210016, P.R. China

Abstract: The main rotor is the lift surface and control surface of a helicopter, and its normal health is crucial for the safety of the helicopter. The rotor fault diagnosis technology is still a weak link in the field of helicopter health and usage monitoring system (HUMS), and the development of rotor fault diagnosis technology is of great value. Based on information fusion technology, the mechanism of rotor failure is analyzed, the rotor failure model is established, and the fault feature information of blades, hub and airframe under different faults are obtained by fluid structure coupled simulation, thus generating data sets for network training and verification. Then genetic algorithm-backpropagation (GA-BP) neural network is used to diagnose three types of helicopter rotor faults, namely, misadjusted trim-tab, misadjusted pitch control rod and imbalanced mass. Three cascaded levels of networks are used to identify fault classification, location and severity, respectively. Finally, the rotor faults are diagnosed and analyzed by the weighted Dempster-Shafer (D-S) evidence theory. The results demonstrate that the rotor blade fault diagnosis method based on the improved D-S evidence theory can be successfully applied to rotor blade fault diagnosis with good identification results.

Key words：rotor system; fault diagnosis; GA-BP neural network; information fusion technology; D-S evidence theory

CLC number：V211.52   **Document code**：A   **Article ID**：1005-1120(2024)01-0066-10

0 Introduction

The helicopter rotor system has complex mechanical structure, more complex aerodynamic and dynamic environment. There are many factors that affect the safety of the rotor system, so that each failure has many causes. Once a fault occurs, it will easily lead to a chain reaction, and then multiple faults will occur concurrently. For example, the aerodynamic imbalance of the rotor blades causes abnormal blade flapping motion, and the dynamic loads at the blade root and hub are too large, which in turn cause the vibration of the airframe to intensify. Its failure rate accounts for a large proportion of helicopter failures, reaching 20%, and 35% of helicopter class-one flying accidents are related to rotor failure[1-2]. Therefore, it is very necessary to study the fault diagnosis technology of helicopter rotor. This is of great significance to improving the reliability of the helicopter, flight safety and reducing maintenance costs[3-4].

The rotor is the lifting and control surface of a helicopter, and the proper functioning of its state is crucial for the safety of the helicopter. Due to the complexity of the rotor's structure and dynamics, it is challenging to obtain real-time fault characteristic signals from the rotor. Therefore, rotor state monitoring and fault diagnosis remain weak areas in the field of helicopters.

In rotor fault diagnosis, information obtained from individual sensors is often limited and may provide a partial view of the system. Moreover, the information collected by sensors is frequently incomplete. Information fusion techniques are employed to process data gathered from multiple sensors, and by separating true data from noise, useful information can be extracted. This enables a comprehensive

---

and multi-dimensional diagnosis of faults from various perspectives. Khazaee et al.[5] conducted the research on fault diagnosis of a planetary gearbox using feature-level acoustic and vibration data fusion. They employed artificial neural networks and the Dempster-Shafer（D-S）evidence theory for this study. Through the information fusion approach, the diagnostic accuracy was enhanced from 88.4% to 98.6%, effectively improving the precision of planetary gearbox fault diagnosis. Azamfar et al.[6] conducted research on gearbox fault diagnosis using a multi-sensor data fusion approach, particularly fusing current signals from electric motors at the data level. They employed convolutional neural networks for this study and validated the effectiveness of multi-sensor data-level fusion in gearbox fault diagnosis.

This paper focuses on information fusion technology to fuse the fault identification results diagnosed according to different fault feature information under the same fault type. Comprehensive and multi-angle fault diagnosis is carried out to further improve the recognition accuracy of rotor fault diagnosis. Information fusion essentially involves the process of synthesizing different bodies of evidence into a new body of evidence within the same recognition framework. This synthesis is achieved using combination rules based on the D-S evidence theory, which can effectively address uncertainties in information fusion.

However, this method has its limitations, particularly when dealing with highly conflicting evidence, it may lead to conclusions that contradict facts. To address this issue, the paper will propose a weighted D-S evidence theory diagnostic model. Based on the evidence distance-weighted evidence combination rule, the weights of the evidence are optimized and allocated. This will effectively reduce evidence conflict and lead to improved fault recognition rates.

1　Analysis of Rotor Failure Mechanism

Aimed at the common types of unbalanced faults of the rotor system, the typical characteristics of the faults in the response of the rotor and the body are found out through theoretical research. The unbalance faults of the rotor system mainly include to the misadjusted trim-tab, misadjusted pitch control rod and imbalanced mass[7]. Through the analysis of the transmission path of rotor fault information, the influence law between fault and response is explored[8]. It lays a theoretical foundation for constructing the mapping relationship between rotor failure and response.

1.1　Rotor failure mode analysis

Fault factors in rotor systems can be primarily categorized into two types. The first type involves changes in the mass distribution of rotor blades, altering the centrifugal force characteristics of the blades. The second type affects the aerodynamic force distribution on either the entire rotor blade or a specific section of the blade, leading to aerodynamic imbalance faults. Therefore, based on these imbalance factors, rotor system faults can be equivalently categorized into three fault modes: trailing-edge flap misalignment, pitch link misalignment, and rotor blade mass imbalance.

1.2　Basis for rotor imbalance fault diagnosis

In the state of helicopter flight, rotor blades maintain balance and undergo deformation due to the combined effects of aerodynamic loads, centrifugal forces, and inertial forces[9]. By placing sensors on the rotor blades, it is possible to acquire data on the stress and deformation of each blade, allowing for the monitoring of their individual states. In the event of a malfunction in one of the blades, the vector of aerodynamic loads, centrifugal forces, and inertial forces acting on that particular blade differs from those acting on the other healthy blades. This discrepancy results in unique stress and deformation patterns in the affected blade compared to the other blades. By analyzing the blade loads, it is possible to diagnose the blade's condition based on changes in its deformation components. This study focuses on diagnosing rotor faults by examining deformation components at the root of the rotor blade.

For an ideal rotor system, the entire rotor remains balance under the influence of aerodynamic forces on each rotor blade and the hub forces. The hub loads, represented as a set of six hub loads or hub six force components, should occur at frequencies that are integer multiples of the product of the number of rotor blades k and the rotor's rotational speed Ω, i.e., $1k\Omega$, $2k\Omega$, $3k\Omega$, and so on[10]. When there is an imbalance fault in one or more rotor blades, the hub loads will exhibit cyclic loading at frequencies of 1Ω, 2Ω, 3Ω, and so forth. Different rotor faults will result in different vibration frequencies of the hub of six force components. By analyzing the hub loads, it is possible to monitor the condition of the rotor blades based on changes in the individual components of the hub loads.

The aircraft maintains balance under the influence of various loads, including hub loads, gravity, and aerodynamic forces. Rotor is the main source of fuselage vibrations, and information about rotor hub and blade vibrations is transmitted to the fuselage, resulting in a corresponding vibration response. Previous research has demonstrated the existence of a one-to-one mapping relationship between the spatial domain of rotor imbalance faults and the multi-point spatial domain of fuselage vibrations. Therefore, it is possible to monitor the condition of the rotor based on the fuselage's vibration signals.

2　Rotor System Modelling

When it comes to identifying faults in rotor systems, gathering a substantial amount of fault characteristic data samples is crucial. The most reliable method is often through flight tests and wind tunnel experiments. However, due to safety and cost considerations, conducting such experiments can be challenging, making it difficult to obtain data for various fault cases. Therefore, this study utilizes simulation software ANSYS to simulate rotor faults and collect fault characteristic data. This approach is cost-effective and versatile, and allows for the simulation of various fault combinations and degrees, making it relatively straightforward to obtain experimental data.

2. 1　Design of rotor parameters

In accordance with the overall design requirements for helicopter rotors, the key rotor system parameters include rotor diameter, blade chord length, number of rotor blades, and rotational speed, among others. This paper focuses primarily on the diagnosis of faults in conventional rotor types. The specific rotor parameters are presented in Table 1.

Table 1　Rotor overall parameters

Parameter	Value
Rotor configuration	Hingeless type
Blade number	4
Rotor radius/m	2
Blade chord/m	0.12
Blade span/m	1.7
Mass of single blade/kg	3.06
Speed/(rad•s^{-1})	95

Aerodynamic design of rotor blades primarily encompasses parameters such as blade twist angle, blade planform shape, and airfoil type. By designing the twist angle of the blades, it ensures that the angle of attack at different radii of the blade is in favorable positions. Given the challenges associated with conducting physical experiments, a rectangular blade planform shape has been chosen in this study. The airfoil type selected for the rotor blades is the OA212 airfoil. The distribution of the blade planform shape and twist angle along the span is illustrated in Fig.1. The three-dimensional model of the rotor blade is illustrated in Fig.2.
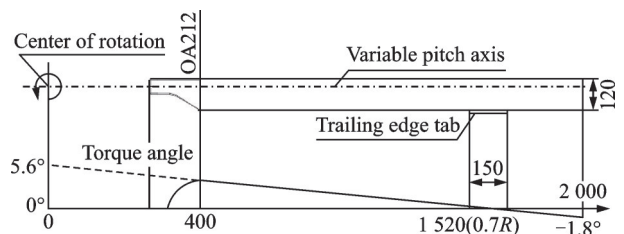

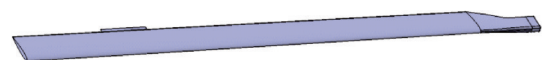Fig.1　Blade planform and twist angle

Fig.2　3-D model of rotor blade

2. 2　Design of propeller hub model

The rotor system utilizes a hingeless rotor hub, primarily composed of the hub central piece, pitch link, pitch change hinge housing, and additional components. The hub central piece experiences substantial loads during rotation. By structurally incorporating pre-coning, a downward centrifugal moment is generated during blade rotation, offsetting the torque caused by blade tension at the root of the hub. This effectively improves the load distribution on the hub.

Following the traditional design pattern and basic structural layout of a hingeless rotor hub, the structural arrangement from the rotor shaft to the blade consists of the following components: The rotor shaft, flexible beams, pitch hinge, and rotor blade. The flexible beam assembly in the hingeless rotor hub comprises the flapwise section and lead-lag section, extending from the rotor shaft towards the rotor blade. The rotor blade is connected to the rotor hub through the pitch hinge. The pitch hinge is linked to the pitch change yoke assembly and the rotating disk. This structure enables pitch change motion of the rotor blades. The rotor hub structure is illustrated in Fig.3.
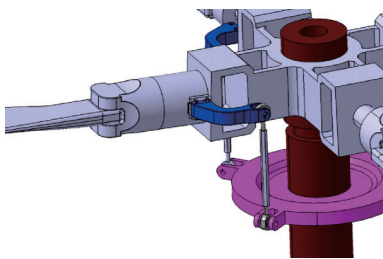
Fig.3　Structure diagram of rotor hub

2. 3　Rotor failure simulation

The rotor system model created in CATIA software is imported into the simulation software ANSYS for fluid-structure interaction (FSI) simulation. The process involves the following steps: Geometry model processing, domain setup, mesh generation, fluid simulation, importing aerodynamic forces into dynamic simulation, solving the computations, and obtaining data.

3　GA-BP Neural Network Model

3. 1　Network construction

Due to the complex structure of rotor systems, simple fault diagnosis methods may struggle to achieve accurate results. The backpropagation (BP) neural network has found extensive application in rotor system fault diagnosis[11]. However, the accuracy of neural networks can significantly decrease when dealing with imprecise or uncertain input information.

To address the issues of low learning efficiency, slow convergence, and susceptibility to converging at local minima associated with traditional BP neural networks, an optimized approach is employed. This involves using a genetic algorithm (GA) to optimize the weights and thresholds of the neural network. This results in an optimized GA-BP neural network, which greatly enhances fault diagnosis accuracy and speed. The GA-BP neural network algorithm is shown in Fig.4.

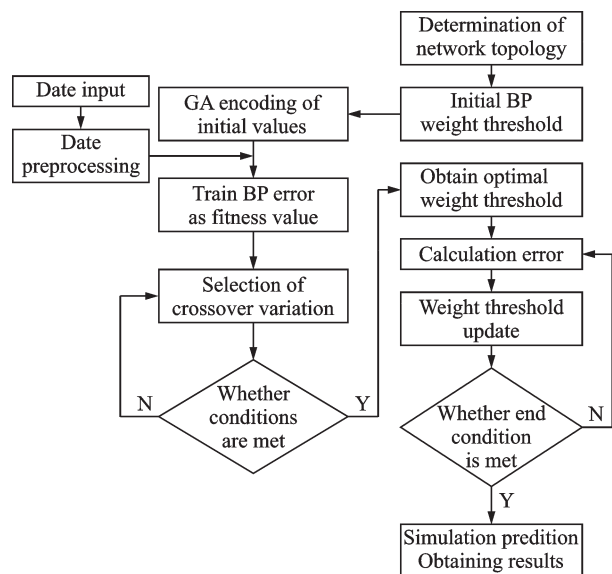Fig.4　GA-BP neural network algorithm flowchart

Three types of fault characteristic signals are extracted from the deformation components of the rotor blades, hub load components, and aircraft vibrations. Based on these three signals, three categories of GA-BP neural network rotor imbalance fault diagnosis models are established. The characteristics of the feature signals are analyzed, and the net-

work structure and parameters for the genetic algorithm are determined within each diagnostic model

category. Simulations are conducted following the fault recognition process as depicted in Fig.5.
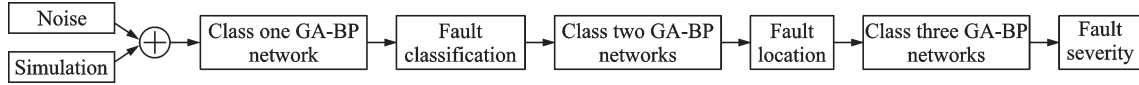

Fig.5　Rotor failure identification flow chart

The fault diagnosis model's genetically optimized BP neural network comprises an input layer, a hidden layer, and an output layer. The first layer is the input layer, with nodes composed of the three types of fault characteristic signals extracted from the deformation components of the rotor blades, hub load components, and aircraft vibrations.

The second layer is the hidden layer, and the nodes in the hidden layer are responsible for extracting relevant features from the input signals. The third layer is the output layer, where nodes correspond to the type of rotor fault, the location of the fault, and the fault severity.

To prevent significant prediction errors resulting from differences in the magnitudes of input and output data, the training data for the neural network is normalized. Based on this normalization, each neural sub-network randomly selects 300 fault data samples for training the fault diagnosis model. The remaining 60 data samples are used to validate the performance of the trained model.

3.2　Fault characteristic quantity (network input)

The rotor system selected for this study is a four-bladed main rotor, and the three types of faults mentioned above will each appear individually on a specific rotor blade. Each type of fault comprises 31 fault levels, ranging from zero to the maximum fault level (including both positive and negative maximum fault levels), incrementally increasing one by one

$$f=\left\{ f|f=-1+k\times\frac{1}{15}\quad k=0,1,\cdots,30\right\} \quad(1)$$

where when $f=0$, it indicates no fault, and when $f=1$ and -1, they represent the maximum fault level in the positive and negative directions. All other numerical values represent fault levels that vary

linearly between zero and the maximum value. Table 2 provides the ranges of variation for the three types of faults.

Table 2　Range of rotor system faults

Fault type	Range of adjustment	f
Misadjusted trim-tab	$-7.5°—7.5°$	$-1—1$
Misadjusted pitch control rod	$8.5°—23.5°$	$-1—1$
Imbalanced mass	$-300g—300g$	$-1—1$

When generating fault data samples, the rotor simulation program's input parameters are adjusted according to the defined fault level values f. This is done to calculate the corresponding rotor responses and obtain fault data samples. The selected fault characteristic signals include deformation components at the root of the rotor blade, hub load components, and aircraft vibrations.

For a four-bladed main rotor, there are 12 characteristic quantities for rotor response, 6 for hub loads, and 18 for fuselage vibration in the horizontal direction. For each type of fault, calculations are performed for 30 fault levels. Therefore, the total number of fault data samples is 1 080. Fig.6 shows the setup of the rotor failure model.

To simulate real-world conditions, noise is added to the simulation results. The "contaminated" results are used as input signals for training the net-
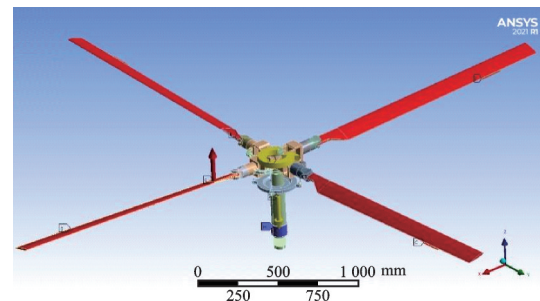

Fig.6　Rotor failure model setup

work[12-13].

In this study, random noise is added to each component p_i of each fault data sample using the following formula to obtain the "contaminated" value p_{ni}, i.e.

$$p_{ni} = p_i(1 + a\varepsilon) \qquad (2)$$

where ε is a random number between -1 and 1 and a the noise level. For example, $a = 0.05$ represents a noise level of 5% in the sample input vector. This paper selects noise level $a = 10\%$.

4 Application of D-S Evidence Theory

Considering at the difficulty of comprehensive evaluation and modeling of helicopter rotor system, it is proposed to use the preliminary diagnosis results of various neural networks as the basis. Change the evaluation factors from high-dimensional features to low-dimensional primary diagnosis results to reduce the complexity of the model. Building upon the classical D-S evidence theory[14-15], a weighted D-S evidence theory model has been introduced. This model optimizes the probability assignment functions by introducing trustworthiness coefficients, effectively reducing evidence conflict and enhancing fault recognition rates.

4.1 Construction of basic probability allocation function

To ensure that the evidence provided by various fault characteristics can be reasonably fused, the key lies in constructing basic probability assignment (BPA) functions based on the existing evidence[16-18]. BP neural networks are known for their strong function approximation capabilities. By using a sigmoid-type activation function in the output layer, the network's output results can be mapped to the [0, 1] interval, allowing the classification results to be output in the form of probabilities. This paper employs the approximation error parameter of the BP neural network to describe the uncertainty of propositions

$$E = \frac{1}{2}\sum_{i=1}^{l}\left(y_i - d_i\right)^2 \qquad (3)$$

where y_i represents the output of the ith neuron, and d_i the expected output result of the ith neuron. The basic probability allocation function of D-S evidence theory is constructed as

$$S = \sum_{j=1}^{l} y(A_i) + E \qquad (4)$$

$$m(A_j) = \frac{y(A_j)}{S} \qquad (5)$$

$$m(\Theta) = \frac{E}{S} \qquad (6)$$

where S represents the total evidence set, $m(A_j)$ the basic probability assignment function for the jth type of fault, and $m(\Theta)$ the basic probability assignment function that describes uncertainty.

4.2 Optimization of D-S evidence theory

This paper proposes a novel weight-based decision-level data fusion method to address the problem of fusing conflicting evidence. The method involves assigning different weights to various sets of evidence to adjust the probability assignment functions. These weights are determined based on the reliability of the evidence.

Assuming you have u sensors and v target types, you will indeed obtain $u \times v$ BPA functions for a particular observed target

$$\begin{bmatrix} m_{11} & m_{12} & \cdots & m_{1v} \\ m_{21} & m_{22} & \cdots & m_{2v} \\ \vdots & \vdots & & \vdots \\ m_{u1} & m_{u2} & \cdots & m_{uv} \end{bmatrix}$$

The basic solution process for weight values is as follows.

(1) Calculate the mean value of u sets of probability distribution functions

$$M_{MED}^j = \frac{1}{u}m \quad i = 1,2,\cdots,u; j = 1,2,\cdots,v_{ij} \qquad (7)$$

(2) Calculate the distance between the basic probability distribution of each group of evidence and the mean value

$$D_i = \sum_{j=1}^{v}\left| m_{ij} - M_{MED}^j \right| \qquad (8)$$

The distance is obtained by accumulating the probability distribution function value of each proposition in a set of evidence with the distance of the corresponding proposition's probability distribution function in the mean value.

（3）Calculate the trust weight of each sensor. For evidence sources that are far from the mean value, they are considered unreliable, and lower trust weights should be assigned. Conversely, for evidence sources that are close to the mean value, they should be assigned higher trustworthiness. Hence, trustworthiness is inversely proportional to the distance. To achieve this, the reciprocal of the distance is computed firstly, i.e.

$$W_i = 1/D_i \qquad (9)$$

Then standardize it as

$$w_i = \frac{W_i}{W_{\max}} \qquad (10)$$

where $W_{\max} = \max W_i$, ensure that the value range of W_i is between [0, 1].

Once the trustworthiness coefficients are determined, the probability assignment functions of the evidence sources are adjusted according to

$$\begin{cases} m_i^*(A) = w_i m_i(A) & A \subset \Theta \\ m_i^*(\Theta) = w_i m_i(\Theta) + 1 - w_i \end{cases} \qquad (11)$$

Following the steps outlined above, evidence is readjusted according to different weights, and the newly obtained basic probability assignment functions are subjected to D-S combination rules for evidence synthesis.

5 Results and Discussion

Fig.7 depicts the fundamental process of rotor fault diagnosis based on the weighted evidence theory. Firstly, fault characteristic information is acquired from three types: rotor responses, hub load, and fuselage vibration. Next, three types of GA-BP neural networks are employed to obtain individual diagnostic results for each type of fault characteristic. These three diagnostic results are then treated as three independent bodies of evidence within the evidence theory framework. Weighted and decision-level fusion is applied to these three sets of evidence, resulting in the final diagnosis.
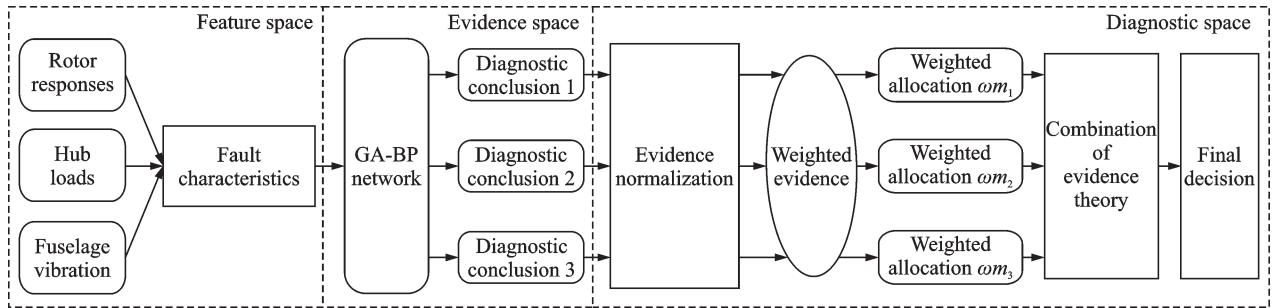

Fig.7   Basic process of rotor fault diagnosis based on weighted evidence theory

5.1 Application of weighted D-S evidence theory in fault type diagnosis

We extracted a set of sample data for each of the three fault types from the experimental samples. Using three different GA-BP network models, we obtained diagnostic output results as shown in Table 3, where f_1 is the trim-tab misadjustment, f_2 the pitch control rod misadjustment, and f_3 the mass imbalance.

For each sample group corresponding to different fault types, the preliminary diagnosis results from three distinct GA-BP network models, based on rotor response, hub loads, and aircraft vibrations as feature signals, are considered as separate sets of

Table 3   Preliminary diagnosis result of a single signal

Diagnostic model	f_1	f_2	f_3	Diagnostic result
Rotor response	0.812 3	0.077 5	0.110 2	f_1
Hub load	0.866 1	0.048 7	0.085 2	f_1
Fuselage vibration	0.236 3	0.389 5	0.374 2	f_2
Rotor response	0.189 1	0.798 3	0.012 6	f_2
Hub load	0.026 4	0.878 3	0.095 3	f_2
Fuselage vibration	0.083 4	0.893 2	0.023 4	f_2
Rotor response	0.032 1	0.035 8	0.932 1	f_3
Hub load	0.052 7	0.1541	0.793 2	f_3
Fuselage vibration	0.046 3	0.108 0	0.845 7	f_3

evidence bodies, denoted as E_1, E_2, and E_3. These evidence bodies are assigned values using the basic

probability functions described in this paper, and the results are presented in Table 4.

Table 4   Assignment of basic probability assignment functions to evidence bodies

Evidence body	$m(f_1)$	$m(f_2)$	$m(f_3)$	Diagnostic result
E_1	0.802 7	0.077 7	0.050 7	f_1
E_2	0.876 7	0.057 2	0.053 9	f_1
E_3	0.229 0	0.235 3	0.224 7	Unknown
E_1	0.183 6	0.774 9	0.012 2	f_2
E_2	0.024 6	0.817 8	0.088 7	f_2
E_3	0.082 7	0.886 3	0.023 2	f_2
E_1	0.032 0	0.035 7	0.929 1	f_3
E_2	0.049 1	0.111 5	0.738 5	f_3
E_3	0.045 5	0.106 2	0.831 7	f_3

From Table 4, it is evident that individual evidence bodies may face situations where uncertainty is too high to make a determination. To address this, the weighted D-S evidence theory fusion method is applied to combine the results of multiple evidence bodies for the same sample. Taking the real condition f_1 as an example, evidence body E_3 cannot identify a specific fault state due to excessive uncertainty in the output results. By synthesizing the three evidence bodies for this sample, the fusion process results are presented in Table 5.

Table 5   Evidence fusion results

Evidence body	$m(f_1)$	$m(f_2)$	$m(f_3)$	Diagnostic result
E_1	0.802 7	0.077 7	0.050 7	f_1
E_2	0.876 7	0.057 2	0.053 9	f_1
E_3	0.229 0	0.235 3	0.224 7	Unknown
E_1&E_2&E_3	0.964 3	0.004 8	0.030 0	f_1

From Table 5, it is apparent that the post-fusion results significantly reduce the probability distribution related to uncertainty and notably increase the probability distribution for the output condition f_1. The application of weighted D-S evidence theory effectively addresses the issue of excessive uncertainty.

5.2   Comparison of results

The utilization of weighted D-S evidence theory in fault location diagnosis and fault degree diagnosis follows a process similar to the one described above, and the ultimate diagnosis results are presented in Tables 6—8.

Table 6   Comparison of fault type diagnosis accuracy

Diagnostic model	Accuracy/%
Based on rotor response	93
Based on hub load	92
Based on fuselage vibration	90
Weighted D-S evidence theory fusion method	98

Table 7   Comparison of fault location diagnosis accuracy

Diagnostic model	Accuracy/%
Based on rotor response	95
Based on hub load	90
Based on fuselage vibration	88
Weighted D-S evidence theory fusion method	96

Table 8   Comparison of fault degree diagnosis accuracy

Diagnostic model	Accuracy/%
Based on rotor response	87
Based on hub load	82
Based on fuselage vibration	79
Weighted D-S evidence theory fusion method	92

Tables 6—8 provide an overall diagnosis accuracy for each method concerning fault type, fault location, and fault degree. Comparing Tables 6 to 8, it becomes evident that relying solely on individual information results in certain errors. However, after applying weighted D-S evidence theory decision-level fusion, the diagnostic accuracy improves. With the weighted D-S evidence theory, accuracy is 98% for fault type diagnosis, 96% for fault location diagnosis, and 92% for fault severity diagnosis.

6   Conclusions

This paper focuses on the research of rotor system fault diagnosis based on three types of fault characteristic signals: Blade deformation, hub load, and aircraft diagnostic signals. Recognizing that the diagnostic accuracy of a single-fault diagnostic mod-

el may not meet practical requirements, this paper combines multiple diagnostic models and proposes a rotor system fault diagnosis method based on weighted D-S evidence theory. The specific research findings are as follows:

(1) For the three rotor faults studied in this paper, three classes of genetic neural networks have been developed to progressively identify fault type, location, and degree.

(2) Experimental results demonstrate that the weighted improved D-S evidence theory not only enhances fault recognition rates but also effectively reduces diagnostic uncertainty.

(3) The ability to identify faults in test samples containing noise has been improved, enhancing network convergence and generalization capabilities.

References

[1] GANGULI R, CHOPRA I, HAAS D J. Helicopter rotor system fault detection using physics-based model and neural networks[J]. AIAA Journal, 2005, 36(6): 1078-1086.

[2] ALKAHE J, RAND O, OSHMAN Y. Damage detection in a rotating helicopter blade using an adaptive estimator[C]//Proceedings of AIAA Guidance, Navigation, and Control Conference and Exhibit. [S.l.]: AIAA, 2000.

[3] GANGULI R, CHOPRA I, HAAS D. Formulation of a helicopter rotor system damage detection methodology[J].Journal of the American Helicopter Society, 1996,41(4): 302-312.

[4] PAWAR P M, GANGULI R. Helicopter rotor health monitoring—A review[J]. Journal of Aerospace Engineering, 2007, 221(5): 631-647.

[5] KHAZAEE M, AHMADI H, OMID M. Feature-level fusion based on wavelet transform and artificial neural network for fault diagnosis of planetary gearbox using acoustic and vibration signals[J]. Insight-Non-destructive Testing and Condition Monitoring, 2013, 55(6): 323-330.

[6] AZAMFAR M, SINGH J, BRAVO-IMAZ I, et al. Multisensor data fusion for gearbox fault diagnosis using 2-D convolutional neural network and motor current signature analysis[J]. Mechanical Systems and Signal Processing, 2020. DOI: 10.1016/j.ymssp.2020.106861

[7] GAO Yadong, DENG Shengping. Unbalance fault identification of helicopter rotor using support vector machine[J]. Journal of Nanjing University of Aeronautics & Astronautics, 2011, 43(3): 435-438. (in Chinese)

[8] GAO Yadong, ZHANG Zengchang. Experimental study of helicopter rotor imbalance fault diagnosis[J]. Journal of Vibration, Measurement and Diagnosis, 2009, 29(2): 214-217,245. (in Chinese)

[9] LIAO Wenfeng, GAO Yadong. Helicopter rotor imbalance fault diagnosis using fuzzy RBF neural network[J]. Journal of Nanjing University of Aeronautics & Astronautics, 2015, 47(2): 285-289. (in Chinese)

[10] XU Yongqin, GAO Yadong, LI Qinglong. Helicopter rotor imbalance fault diagnosis method based on wavelet transform and neural network[J]. Journal of Nanjing University of Aeronautics & Astronautics, 2017, 49(2): 212-218. (in Chinese)

[11] WANG Linjun, HUANG Wenchao, ZHONG Xianyou, et al. Fault diagnosis method for rolling bearing based on GA-BP algorithm and EMD[J]. Coal Mine Machinery, 2019, 40(5): 167-170. (in Chinese)

[12] YANG Mao, LI Xiaolong. Fault identification of rotor system based on simulation data[J]. Journal of Zhejiang University (Engineering Edition), 2013, 47(12): 2188-2194. (in Chinese)

[13] LIU Hongmei, LYU Chen, HOU Wenkui, et al. Fault diagnosis of helicopter rotor system based on support vector machine[J]. Journal of Huazhong University of Science and Technology (Natural Science Edition), 2009, 37(S1): 151-155. (in Chinese)

[14] DEMPSTER A P. Upper and lower probabilities induced by a multivalued mapping[J]. The Annals of Mathematical Statistics,1967,38(2): 325-339.

[15] SHAFER G A. A mathematical theory of evidence[M]. Princeton, New Jersey: Princeton University Press, 1976.

[16] LI Ping. Fault diagnosis method of rotating machinery based on fusion of multiple vibration signal information[D]. Xiangtan: Hunan University of Science and Technology, 2008. (in Chinese)

[17] MO Qi, SUN Guoxi. Application of information fusion technology in fault diagnosis of rotating machinery[J]. Manufacturing Automation, 2010, 32(4): 76-77,110. (in Chinese)

[18] XU Tongle. Research on fault diagnosis method of rotating machinery based on fusion of multiple sensor information[D]. Beijing: Beijing University of Posts and Telecommunications, 2012. (in Chinese)

Author　　Dr. **GAO Yadong** studied in Nanjing University of Aeronautics and Astronautics, majoring in aircraft design, and obtained the B.S., M.S. and Ph.D. degrees in 1997, 2000 and 2004, respectively. From March 2004 to October 2006, he worked as a postdoctoral fellow in mechanical engineering. From November 2006 to present, he has been teaching in National Key Laboratory of Rotorcraft Aeromechanics. From January 2012 to January 2013, he worked as a visiting scholar in Aeronautical Composite Structure Research Center, University of Nottingham. From April 2019, he served as Director of Department of Helicopter and Deputy Director of Rotorcraft Aeromechanics.

Author contributions　　Dr. **GAO Yadong** designed the study. Mr. **ZHANG Chuanzhuang** wrote the original manuscript, contributed to the discussion and background of the study and revised the final manuscript. All authors commented on the manuscript draft and approved the submission.

Competing interests　　The authors declare no competing interests.

（Production Editor：SUN Jing）

基于加权 D-S 证据理论的旋翼故障诊断

高亚东，张传壮

（南京航空航天大学航空学院,南京 210016,中国）

摘要：旋翼作为直升机的升力面和操作面,其健康状态对直升机的安全至关重要。旋翼故障诊断技术仍是直升机健康与使用监测系统(Health and usage monitoring system, HUMS)领域的薄弱环节,开发旋翼故障诊断技术具有重要价值。基于信息融合技术,首先分析了旋翼故障的诊断机理,建立了旋翼故障模型,通过流固耦合仿真获取了不同故障下桨叶、轮毂和机身的故障特征信息,生成数据集进行网络训练和验证。然后,利用遗传算法反向传播(Genetic algorithm-backpropagation, GA-BP)优化神经网络诊断3种类型的直升机旋翼故障,即后缘调整片误调、变距拉杆误调和桨叶质量不平衡。3个逐级神经网络分别对旋翼故障类型、故障位置和故障程度进行了诊断识别。最后采用加权的Dempster-Shafer(D-S)证据理论对旋翼故障进行诊断和分析。结果证明基于改进D-S证据理论的旋翼故障诊断方法能够成功应用到旋翼故障诊断中,并具有良好的识别效果。

关键词：旋翼系统;故障诊断;GA-BP神经网络;信息融合技术;D-S证据理论